24th INTERNATIONAL CONGRESS ON SOUND AND VIBRATION
23–27 July 2017, London

REMOTE ACOUSTIC SENSING OF BOUNDARY DEFECTS IN A PLATE IN A MULTIPATH ENVIRONMENT WITH KNOWN OR UNKNOWN INPUT FORCING

Tyler J. Flynn *and* David R. Dowling

University of Michigan, Ann Arbor, Michigan, United States
email: tjayflyn@umich.edu

Acoustic radiation from a mechanical structure due to broadband forcing may be described by a frequency response function (FRF) if the forcing waveform is known. This FRF is dependent on the structure's material, geometry, and boundary conditions and changes to these mechanical properties can result in detectable changes to the FRF. Even if the input forcing is unknown, time-domain cross-correlation methods can be used to detect differences in remote acoustic recordings compared to baseline measurements collected in the absence of mechanical changes. In either case, collecting suitable remote acoustic measurements may be difficult in a reverberant environment due to the detrimental effects of multipath. Here, experimental results are presented for remote acoustic detection of mechanical changes to a vibrating 0.3-m-square by 3-mm-thick aluminium plate in a reverberant environment. The plate has nominally clamped edges and is subjected to swept-frequency base excitation. Sound from the plate is recorded remotely with a 15 microphone array with varying levels of plate-boundary defects simulated by altering the clamping configuration at the plate's edges. These array recordings are then processed using Synthetic Time Reversal to reconstruct the radiated sound signal corrected for the environment's unknown reverberation. These reconstructed signals are used to compute FRFs in the case of known input forcing, and compared directly in the case of unknown input forcing. The effectiveness of both approaches is compared for the detection of simulated boundary defects. [Sponsored by NAVSEA through the NEEC, and by the US DoD through an NDSEG Fellowship]

Keywords: Remote, Sensing, SHM, Detection, Plates

1. Introduction

When a mechanical structure is damaged or otherwise mechanically changed, its vibrational characteristics are subsequently affected[1,2]. If the structure is in a fluid medium, such alterations in vibratory behavior likewise result in changes to the sound radiated from the altered structure[3]. The radiated sound can be recorded using passive receivers to gather insight into the health of the structure. In particular, if a baseline measurement of a "healthy" structure can be collected, future measurements may be compared to the baseline for classification as changed or unchanged. *Remote* acoustic detection provides benefits over other popular methods of damage detection – such as vibration monitoring[4-6], acoustic emissions testing[7,8], and nearfield acoustic holography[9,10] – in that it is truly remote and non-contact. While these methods are certainly powerful tools, there are significant drawbacks associated with requiring transducers to be near or in contact with a test structure. Challenges include difficulty of installation, infeasibility of in situ measurements, aging and failing transducers, and unexpected effects of physical coupling between transducers and test structures.

While remote acoustic structural health monitoring (SHM) avoids many of the issues associated with transducer placement, it does require accurate signal identification which can be difficult in real-world environments due to unknown environmental factors like noise, acoustic

environment uncertainty, and multipath propagation[11]. Multipath presents a particular difficulty as the desired broadcast signal is convolved with the environmental Green's function which is generally unknown, and conventional techniques are incapable of inverting this operation. However, once signal identification is achieved, there are many ways of quantifying the differences between baseline and test measurements, the choice of which may affect the performance of a detection test. In certain scenarios, one may even know the a structure's input forcing which can be leveraged by computing a Frequency Response Function (FRF) to gain further insight[4].

In this paper, small mechanical changes in a vibrating plate are detected using remote acoustic array data collected in an unknown reverberant environment. A method of blind deconvolution is used to reconstruct the plate's radiated acoustic signature in spite of strong reverberation. Various metrics are then used to quantitatively compare baseline "healthy" plate measurements, to those of potentially changed plates. The benefits of knowing input forcing, and the FRF, are investigated and compared to tests when input forcing is not considered. Detection performance of the various approaches is quantified and summarized using common detection statistics.

2. Methodology

2.1 Experimental Setup

The experimental apparatus is shown in Fig. 1. The radiating test structure consists of a clamped 30 x 30 x 0.3 cm aluminum plate clamped along all sides to a rigid aluminum base. Eight-second-duration linear frequency sweeps from 100-2000 Hz are created on a computer and sent through a DAC to a Modal Shop K2007E01 series electrodynamic shaker providing input forcing to the rigid test base. The exact input forcing is simultaneously recorded using a PCB 208C01 inline force transducer. Sound from the resulting plate vibration is then radiated into the laboratory environment and recorded at a vertical microphone array with 2-inch spacing between the 15 PCB 130E20 receivers (total aperture of 0.7 m). The array data are then band-passed filtered, and sent to a National Instruments PXIe-6368 ADC system. The input forcing bandwidth is chosen to encompass approximately the first dozen vibrational modes of the test plate.

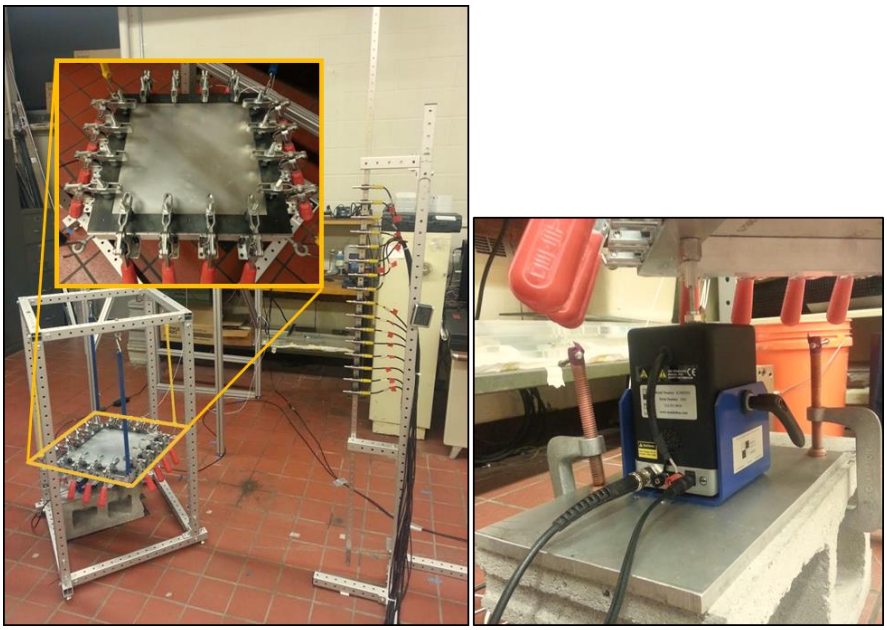

Figure 1: Experimental setup with plate apparatus and 15 receiver vertical array in the test environment (left) and 7 lbf shaker providing base excitation of the plate (right). A detailed view of the plate and clamping geometry is shown at top left.

Mechanical changes were introduced to the test plate by disengaging select clamps at the plate edge, thereby modifying the boundary conditions representative of fastener or weld failure.

Two test cases were considered: a single clamp disengaged near the center of the plate edge and a single clamp disengaged near a corner, a less vibrationally active region. In addition, measurements of a fully clamped "healthy" plate served as a baseline against which to test the detection metrics. The various clamping configurations are detailed in Fig. 2.

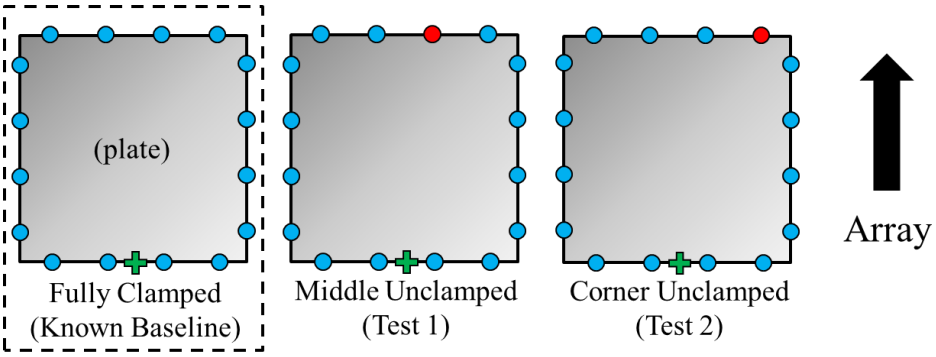

Figure 2: Plate Clamping geometry for the two test cases and baseline. Blue and red circles represent fully engaged and dis-engaged clamps. Green pluses (+) indicate the location of the input forcing at the base.

The testing environment consists of an approximately 24 x 25 ft laboratory space at the University of Michigan which provided a reverberant environment with a T_{60} time of about 0.5 sec. The extent of reverberation is quantified by the signal-to-reverberation ratio (SRR) defined

$$SRR \equiv 10 \log_{10} \left(\frac{SE_{\text{Direct}}}{SE_{\text{Reverb}}} \right) \tag{1}$$

where SE_{Direct} and SE_{Reverb} are the signal energies of the direct path and all-other-paths portions of the signal, respectively. The SRR is a function of plate position in the room (fixed for all measurements) and the array location. For each array location, the SRR was measured by substituting a simple home audio speaker for the plate apparatus, and broadcasting a 100-2000 Hz linear chirp that was recorded by a single receiver at the array center. Reference measurement of the broadcast signal allowed for a matched filter to be applied to these reverberation data, from which SE_{Direct} and SE_{Reverb} were computed. This additional filtering step was required as the broadcast signals – on the order of seconds – were far too long to be truncated in time.

2.2 Synthetic Time Reversal

Synthetic Time Reversal (STR) was used to estimate the vibrating plate's original broadcast acoustic signature from acoustic measurements in the reverberant laboratory *without* a priori knowledge the original waveform. STR is an existing blind deconvolution method which is fast, has a low computational cost, and requires no a priori knowledge of source or array location[12].

The mathematical details of STR have been discussed previously[12] and are omitted for brevity. Ultimately, for an M receiver array with Fourier transformed receiver outputs $\hat{P}_j(\omega)$, STR estimation of a broadcast signal is accomplished by selecting weighting vectors $W_j(\omega)$ such that a surrogate Green's function can be constructed for each receiver using only the recorded waveforms. The surrogate Green's functions are then used to synthetically backpropagate the original array recordings, thereby providing an estimate of the original broadcast signal. Conveniently, it has been shown that the weights $W_j(\omega)$ required for this operation are the same weights computed from conventional beamforming techniques[13]. The Fourier transform of the estimated signal is then given by

$$\hat{S}_{est}(\omega) = \left\{ \sum_{j=1}^{M} \hat{P}_j(\omega) e^{-i\alpha(\omega)} \Big/ \sqrt{\sum_{k=1}^{M} \left| \hat{P}_k(\omega) \right|^2} \right\}^* \hat{P}_j(\omega) \tag{2}$$

where $\alpha(\omega)$ is a phase factor given by

$$\alpha(\omega) = \arg\left(\sum_{j=1}^{M} W_j(\omega)\,\hat{P}_j(\omega)\right) \tag{3}$$

2.3 Detection Metrics

With STR-reconstructed signals for baseline and test cases in hand, three metrics were used to quantify change between the signals. Each detection metric is the function of one test measurement and one baseline, resulting in a scalar value. To statistically evaluate detection performance a batch of eight acoustic array measurements was collected for each of the two partially unclamped test cases and two batches of eight array measurements were collected for the fully clamped baseline. Every pair-wise combination of reconstructed signals was evaluated using one of the metrics outlined below. Metrics were computed between the two test case batches and *one* of the baseline batches, and similarly the two baseline batches were evaluated against one another. This ultimately yielded three sets of 64 detection metric samples (one set for both test cases, and one for the baseline), which were binned into histograms and used to statistically quantify detection performance. A flowchart of the detection procedure is provided in Fig. 3.

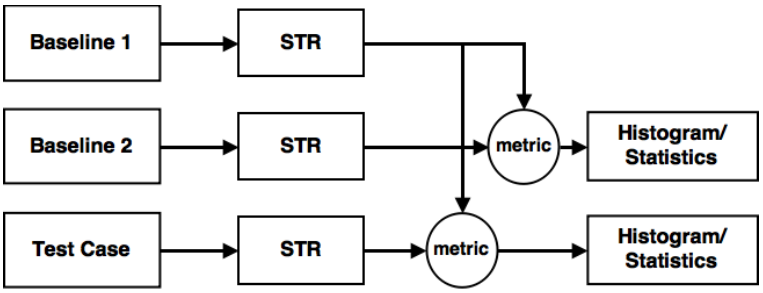

Figure 3: Procedural flow chart for the statistical evaluation of structural health using a comparative metric between remote acoustic test and baseline measurements. This can be extended to an arbitrary number of test cases, though two were considered in this study.

2.3.1 Time Domain Correlation

Perhaps the most straight-forward method of evaluating the difference between two signals is time domain cross correlation. In this case, the metric for baseline measurement $b(t)$ and test measurement $s(t)$ is

$$\Delta_{TD} = \max_{\tau} \frac{\int_{-\infty}^{\infty} b(t)s(t+\tau)dt}{\sqrt{\int_{-\infty}^{\infty} b(t)^2 dt}\sqrt{\int_{-\infty}^{\infty} s(t)^2 dt}} \tag{4}$$

which is bounded between zero and unity.

2.3.2 Power Spectrum Correlation

Changes in stiffness or mass distribution due to damage in a structure are likely to result in changes in frequency response[1]. Such changes are captured in the power spectrum of a signal. As such, the second detection metric is the frequency domain correlation between the power spectral density (PSD) of the baseline and test measurements

$$\Delta_{PSD} = \max_{\omega'} \frac{\int_{-\infty}^{\infty} \left|\hat{b}(\omega)\right|^2 |\hat{s}(\omega+\omega')|^2 d\omega}{\sqrt{\int_{-\infty}^{\infty} \left|\hat{b}(\omega)\right|^4 d\omega}\sqrt{\int_{-\infty}^{\infty} |\hat{s}(\omega)|^4 d\omega}} \tag{5}$$

where $\hat{b}(\omega) = \int_{-\infty}^{\infty} b(t)e^{i\omega t}dt$ and $\hat{s}(\omega)$ follows similarly.

2.3.3 *Frequency Response Function Correlation*

If the input forcing function $f(t)$ is known, then the acoustic FRF at the array can be calculated. FRF's are convenient functions as they contain the same beneficial structural frequency information as the power spectra, however the FRF are independent of changes or variation in the input forcing. The detection metric using frequency response is

$$\Delta_{FRF} = \max_{\omega'} \frac{\int_{-\infty}^{\infty} FRF_b(\omega) * FRF_s(\omega + \omega')d\omega}{\sqrt{\int_{-\infty}^{\infty} FRF_b(\omega)d\omega}\sqrt{\int_{-\infty}^{\infty} FRF_s(\omega)d\omega}} \tag{6}$$

where $FRF_b(\omega)$ and $FRF_s(\omega)$ are the frequency response functions computed for the baseline and test cases, respectively, and defined as

$$FRF_b(\omega) = \left|\frac{\hat{b}(\omega)}{\hat{f}(\omega)}\right| \tag{7}$$

3. Results

Metrics were computed for the receiver array at 1 meter (SRR = –7dB) from the radiating plate and are shown in Fig. 4. The three batches of coefficients (test case 1 to baseline, test case 2 to

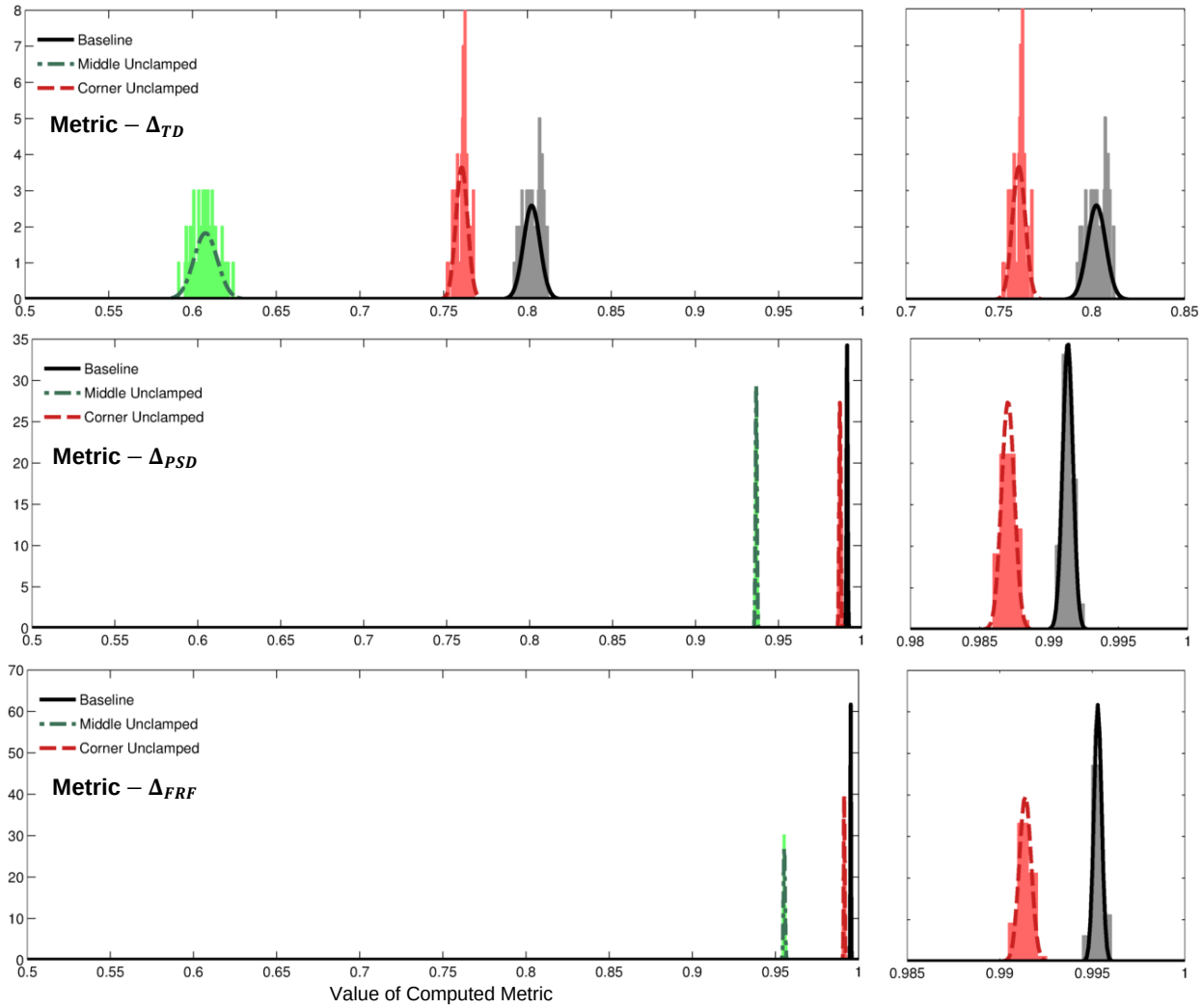

Figure 4: Sets of histograms and Gaussian fits using the Time Domain Correlation (top), PSD Domain Correlation (center), and FRF Correlation (bottom) at 1 m range. Enhanced views of the Test Case 2 (corner unclamped) and baseline (fully clamped) histograms are shown to the right.

baseline, and baseline to baseline) were binned into three histograms, and plotted on the same abscissa. These results can be assessed by the fact that histograms that are more greatly separated, correspond to better detection performance, i.e. there is little chance of mischaracterizing a test case for a baseline case (type I error) or vice-versa (type II error). The absolute location of the histograms on the abscissa is also important. While the relative separation between baseline and test case histograms are necessary for evaluating detection performance, using a metric that results in a baseline histogram that is very near unity is also beneficial in that it may eliminate the need to collect baseline measurements at all. For example, when using the Δ_{TD} metric, it is clear that some knowledge of the system is necessary, otherwise a user might erroneously claim that a test consistently resulting in Δ_{TD} = 0.8 is suspected unhealthy, even though it lies squarely in the baseline histogram, as shown at the top of Fig. 4, and is *not* representative of plate-edge change. Conversely, using the Δ_{PSD} or the Δ_{FRF} metrics, any test yielding a value less than 0.98 is very likely suspect for plate edge unclamping or some other mechanical change.

For comparison, this procedure was repeated without applying STR to the array data. Two additional approaches were considered, conventional spherical wave beamforming, and simply using no post-processing with just a single receiver. Results of these tests using the Δ_{TD} metric are shown in Fig. 5. The significant overlapping of the baseline and test case 2 histograms indicate that neither method performed as well as STR in differentiating the corner unclamped and fully clamped cases. Similar results were found using the Δ_{PSD} and Δ_{FRF} metrics with the alternative methods. These findings indicate that the implementation of STR aids in reducing variability of the compared signals due to reverberation, thereby making variability due to mechanical changes in the plate apparatus more detectable.

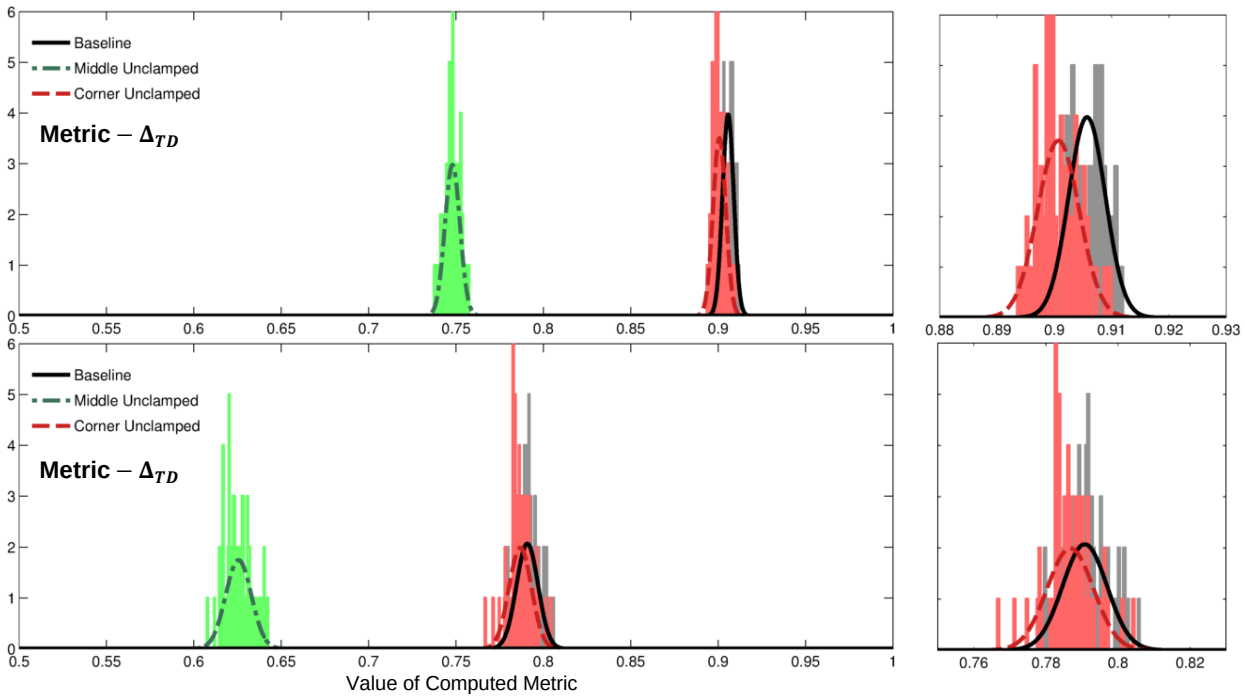

Figure 5: Sets of histograms and Gaussian fits using the Time Domain Correlation metric on a single unprocessed receiver (top) and a conventional beamformer output (bottom).

Additional results using STR were further quantified by fitting the histograms with normal distributions. Given that each fit has an associated mean μ and standard deviation σ, a detection index d can be defined

$$d = \frac{\mu_b - \mu_s}{\sigma_s} \tag{8}$$

where subscripts b and s correspond to baseline and test case, respectively. Given that the standard deviations of the distributions are of similar size, the detection index acts as a measure of resolvability between two distributions and is a convenient metric for detection performance[14]. Values of μ_b and d are tabulated for each detection metric for at three array ranges in Table 1.

		Time Domain Correlation			PSD Correlation			FRF Corerelation		
Range	SRR	$\mu_{Baseline}$	d_{Center}	d_{Corner}	$\mu_{Baseline}$	d_{Center}	d_{Corner}	$\mu_{Baseline}$	d_{Center}	d_{Corner}
1 m	-7 dB	0.80	39.5	13.5	0.99	48.0	13.7	0.995	63.0	18.9
2 m	-11 dB	0.86	36.8	12.2	0.98	34.4	9.8	0.998	53.3	15.2
3 m	-13 dB	0.89	34.3	9.8	0.99	39.7	6.9	0.993	59.5	9.6

Table 1: Mean baseline value and detection indexes for each detection metric. Tests were performed with the receiver array at 1 m, 2 m, and 3 m from plate center.

4. Summary and Conclusions

Remote acoustic array measurements were shown to be effective in detecting mechanical changes in a vibrating plate in a reverberant laboratory using a blind deconvolution algorithm. Using synthetic time reversal, estimates of the plate's acoustic signature were computed from raw array recordings corrupted by unknown multipath and reverberation. These reconstructed signals were then used to classify the vibrating plate as either changed or unchanged, using either correlation between the time series, PSDs, or Frequency Response Functions as detection metrics. All three metrics were effective in discriminating a fully clamped plate from a plate with a single clamp disengaged. Of these metrics, correlation of the Frequency Response Function was found to be the best option both in its ability to distinguish between baseline and test cases and the near-unity values for baseline-baseline comparisons. While Frequency Response Functions were found to be better than time series and PSDs in detecting changes, the metric necessitates knowledge of the input forcing into the structure. While in some cases input forcing could be measured or estimated – for example, vibrations due to cyclical loading of a bearing or forces from the prime mover on a shipping vessel – in general it is not known. In lieu of knowledge about the input forcing, using the signal PSDs was also an effective metric. Additionally, frequency based approaches feature the potential benefit of independence from signal phase, meaning that they would likely be promising for applications where uncorrelated, broadband noise-like input forcing drives the vibration.

REFERENCES

1 Balageas, D., Fritzen, C. P., and Güemes, A. Eds., *Structural Health Monitoring*. Vol. 90, John Wiley & Sons (2010).

2 Carden, E. P., and Fanning, P. Vibration Based Condition Monitoring: A Review, *Structural Health Monitoring* **3**(4), 355-377, (2004).

3 Junger, M. C., and Feit, D., *Sound, Structures, and Their Interaction*. Vol. 225, MIT press, Cambridge, MA (1986).

4 Montalvao, D., et al. A Review of Vibration-Based Structural Health Monitoring with Special Emphasis on Composite Materials, *Shock and Vibration Digest* **38**(4), 295-324, (2006).

5 Salawu, O. S. Detection of Structural Damage through Changes in Frequency: A Review, *Engineering Structures*, **19**(9), 718-723, (1997).

6 Sohn, H., and Farrar, C. R. Damage Diagnosis Using Time Series Analysis of Vibration Signals, *Smart Materials and Structures*, **10**(3), 446-451, (2001).

7 Kessler, S. S., Spearing, S. M. and Soutis, C. Damage Detection in Composite Materials Using Lamb Wave Methods, *Smart Materials and Structures*, **11**(2), 269-278, (2002).

8 Raghavan, A., and Cesnik, C. E. S. Review of Guided-Wave Structural Health Monitoring, *Shock and Vibration Digest*, **39(**2), 91-116, (2007).

9 Maynard, J. D., Williams, E. G. and Lee, Y. Nearfield Acoustic Holography: I. Theory of Generalized Holography and the Development of NAH, *The Journal of the Acoustical Society of America*, **78**(4), 1395-1413, (1985).

10 Wenbo, L., et al. A Fault Diagnosis Scheme of Rolling Element Bearing Based on Near-Field Acoustic Holography and Gray Level Co-Occurrence Matrix, *Journal of Sound and Vibration*, **331**(15), 3663-3674, (2012).

11 Stojanovic, M., and Preisig, J. Underwater Acoustic Communication Channels: Propagation Models and Statistical Characterization, *IEEE Communications Magazine*, **47**(1), 84-89, (2009).

12 Sabra, K. G., and Dowling, D. R. Blind Deconvolution in Ocean Waveguides Using Artificial Time Reversal, *The Journal of the Acoustical Society of America*, **116**(1), 262-271, (2004).

13 Abadi, S. H., Rouseff, D. and Dowling, D. R. Blind Deconvolution for Robust Signal Estimation and Approximate Source Localization, *The Journal of the Acoustical Society of America* **131**(4), 2599-2610, (2012).

14 Urick, R. J., and Gaunaurd, G. C. Technical Report NOLTR-72-47, Detection of Fluctuating Sonar Targets, Naval Ordnance Lab, White Oak MD, (1972).